HAL
archives-ouvertes.fr

Joint assimilation of surface soil moisture and LAI observations into a land surface model

Joaquín Muñoz Sabater, Christoph Rüdiger, Noureddine Fritz,
Jean-Christophe Calvet, Lionel Jarlan, Yann Kerr

▶ **To cite this version:**

Joaquín Muñoz Sabater, Christoph Rüdiger, Noureddine Fritz, Jean-Christophe Calvet, Lionel Jarlan, et al.. Joint assimilation of surface soil moisture and LAI observations into a land surface model. Agricultural and Forest Meteorology, Elsevier Masson, 2008, 148, pp.1362-1373. <10.1016/j.agrformet.2008.04.003>. <meteo-00348124>

HAL Id: meteo-00348124
https://hal-meteofrance.archives-ouvertes.fr/meteo-00348124

Submitted on 17 Dec 2008

HAL is a multi-disciplinary open access archive for the deposit and dissemination of scientific research documents, whether they are published or not. The documents may come from teaching and research institutions in France or abroad, or from public or private research centers.

L'archive ouverte pluridisciplinaire **HAL**, est destinée au dépôt et à la diffusion de documents scientifiques de niveau recherche, publiés ou non, émanant des établissements d'enseignement et de recherche français ou étrangers, des laboratoires publics ou privés.

JOINT ASSIMILATION OF SURFACE SOIL MOISTURE AND LAI OBSERVATIONS INTO A LAND SURFACE MODEL

Joaquín Muñoz Sabater, Christoph Rüdiger, Jean-Christophe Calvet, Noureddine Fritz,

CNRM-GAME, Météo-France / CNRS, Toulouse, France

Lionel Jarlan

and Yann Kerr

CESBIO, Toulouse, France

ABSTRACT

Land Surface Models (LSM) offer a description of land surface processes and set the lower boundary conditions for meteorological models. In particular the accurate description of those surface variables which display a slow response in time, like root zone soil moisture or vegetation biomass, is of great importance. Errors in their estimation yield significant inaccuracies in the estimation of heat and water fluxes in Numerical Weather Prediction (NWP) models. In the present study, the ISBA-A-g_s LSM is used decoupled from the atmosphere. In this configuration, the model is able to simulate the vegetation growth, and consequently LAI. A simplified 1D-VAR assimilation method is applied to observed surface soil moisture and LAI observations of the SMOSREX site near Toulouse, in south-western France, from 2001 to 2004. This period includes severe droughts in 2003 and 2004. The data are jointly assimilated into ISBA-A-g_s in order to analyse the root zone soil moisture and the vegetation biomass. It is shown that the 1D-VAR improves the model results. The efficiency score of the model (Nash criterion) is increased from 0.79 to 0.86 for root-zone soil moisture and from 0.17 to 0.23 for vegetation biomass.

contact address:
Jean-Christophe Calvet, CNRM-GAME, Météo-France/CNRS,
42, avenue G. Coriolis, 31057 Toulouse Cedex 1, France.
e-mail: jean-christophe.calvet@meteo.fr

1. Introduction

The Land Surface Models (LSM) used in meteorology have been developed in order to simulate continuous land surface processes, such as plant transpiration, soil evaporation and the evolution of soil moisture and surface temperature at regional and global scales. A number of CO_2-responsive LSMs, like the ISBA-A-g_s model of Météo-France (Calvet et al. 1998, Calvet et al. 2004, Gibelin et al. 2006), are able to simulate photosynthesis and plant growth. In particular, the vegetation biomass and the leaf area index (LAI) evolve dynamically in response to climate conditions. These models allow the assimilation of soil moisture and LAI observations.

In the present study, two variables with significant impact on the heat and water fluxes are considered: root zone soil moisture (w_2) and above-ground vegetation biomass (*Bio*). Soil moisture regulates the partitioning between latent and sensible heat fluxes, which has a significant influence on the amount of cloud formation, air temperature, and humidity, among others (Segal et al., 1995, Shaw et al., 1997, Seuffert et al., 2002). At the same time, vegetation biomass plays a very important role in the exchange of water vapor and CO_2 between the vegetation canopy and the atmosphere. All aforementioned variables are key input variables into Global Circulation Models (GCM) (Chase et al, 1996, Bounoua et al, 2000). However, as a consequence of different model complexities and surface parameterizations, there is a range of uncertainty in the simulation of these variables by LSMs (Henderson-Sellers et al., 1993, Henderson-Sellers et al., 1995, International GEWEX Project Office, 1995). Data assimilation systems allow to integrate the rich information provided by remotely sensed surface variables into LSMs, in order to improve the model predictions (eg. Entekhabi et al., 1994; Houser et al., 1998, Lakshmi and Susskind, 2001). To achieve this, LSMs are coupled with Radiative Transfer Models (RTM) to relate remotely sensed quantities to land-surface variables. For example, the L-Band Microwave Emission of the Biosphere (L-

MEB) model (Wigneron et al., 2005) relates L-band brightness temperatures to surface soil moisture (w_g) variations. w_g products are already available at global scale through instruments such as the Advanced Microwave Scanning Radiometer for EOS (AMSR-E) sensor (Njoku et al, 2003) or those that will be provided in L-band by the future Soil Moisture and Ocean Satellite (SMOS) mission of the European Space Agency (ESA) (Kerr et al., 2001). These observations can be used to analyze w_2 (Entekhabi et al., 1994, Reichle et al., 2001). Additionally, a large quantity of satellite-derived LAI products is available, such as those from the MODerate-Resolution Imaging Spectroradiometer (MODIS) at 1 km spatial resolution (Tian et al. 2002a, Tian et al. 2002b, Tan et al. 2005) or the POLarization and Directionality of Earth Reflectances (POLDER) sensor (Bicheron and Leroy, 1999, Roujean and Lacaze, 2002). LAI observations have been shown to be useful for the analysis of the vegetation biomass (Cayrol et al., 2000).

This paper is a continuation of the study of Muñoz Sabater et al. (2007) (henceforth called MU07). In MU07, w_g observations were assimilated using four different assimilation approaches. The simplified 1D-VAR method demonstrated to be the most suitable for an implementation in an operational configuration. Although the results for the w_2 analyses were generally satisfactory, the LSM was forced with a prescribed LAI obtained from in-situ measurements. In the present paper, a step forward is made, and the LAI is simulated by the surface scheme using the parameterization for the plant photosynthesis and growth model of ISBA-A-gs (Gibelin et al. 2006). The main objective is the analysis of w_2 and vegetation biomass through the joint assimilation of LAI and w_g observations. The experimental data originates from the SMOSREX experimental site (De Rosnay et al., 2006). The period under investigation extends over four years from 2001 to 2004, during which very contrasting meteorological conditions were observed.

In section 2, the experimental site, the data set, the ISBA-A-g_s LSM, and the data assimilation scheme are described. Also, the choice of the assimilation parameters is discussed through sensitivity and Monte-Carlo based methods. In section 3, the results are presented for the 4-year period and discussed for two configurations of the assimilation (fixed and time-variant wilting point) and for different accuracies of the atmospheric forcing. Finally, section 4 discusses and summarizes the main conclusions.

2. Methodology

2.1. Experimental site and data set

The SMOSREX site is situated within the ONERA (French National Aerospace Research Establishment) centre of Fauga-Mauzac, located 40 km south-west of Toulouse (43º23'N, 1º17'E, 188 m altitude). SMOSREX (De Rosnay et al., 2006) is a field scale experiment, operative since 2001. In this study, the southern part of the site, covered by vegetation (natural fallow) is studied. An estimation of w_g is obtained through the measurements provided by four probes (ThetaProbe, Delta T Devices) vertically installed at the surface at different locations within the experimental field site. They provide continuous observations over the first 6 cm of the soil surface layer. Daily mean w_g^j values are obtained by averaging the measurements of the four probes and their standard deviation permits to estimate the uncertainty of the observations. The root-zone soil moisture is obtained by calculating an average bulk soil water content from the surface probes and additional soil moisture sensors horizontally installed at depths of 10, 20, 30, 40, 50, 60, 70, 80 and 90 cm. From the individual measurements, a mean and a standard deviation are computed on a daily basis, and the daily standard deviation averaged over the year 2001 is assumed to represent the observation error: $\sigma(w_g^{OBS}) = 0.03\ \ m^3 m^{-3}$ and $\sigma(w_2^{OBS}) = 0.02\ \ m^3 m^{-3}$. Due to a lack of sufficient spatial sampling at the field site, the spatial averaging is replaced by a temporal one (ergodicity principle). These uncertainties are attributed to the moisture observations in subsequent years (2002-2004). The atmospheric forcing (precipitation, atmospheric pressure, wind speed and direction, air humidity, air temperature, and incident solar and infrared radiation) is obtained from a meteorological station at the field site performing continuous measurements, obtained every minute and averaged at 30 minute intervals.

Manual measurements of the vegetation characteristics (LAI, above-ground biomass and necromass, height of the canopy) were generally carried out every two weeks. The LAI and above-ground biomass/necromass measurements were performed by harvesting random sample areas of 25 x 25 cm^2 (4 replicates), and using planimetric and gravimetric methods. For each sample, green biomass and dead plant material were measured separately (De Rosnay et al. 2006). Fig. 1 shows the in-situ observations of the LAI, the surface and root-zone soil moisture and the monthly accumulated precipitation for the four years (2001-2004). It is shown that 2003 was a particularly dry year, with an annual cumulative precipitation of less than 600 mm. Unlike the other years, 2003 shows an atypical double cycle of LAI, with a first peak in spring and a second one at the beginning of the winter season. Precipitation is quite irregularly distributed during 2004, with a wet spring and a very dry summer. This causes a rapid growth of the vegetation and a marked senescence during the dry period, with moisture observations reaching values below the wilting point (w_{wilt}) throughout the summer and part of autumn.

In Table 1 a list of the most relevant characteristics of the soil at the SMOSREX site for ISBA-A-g_s is provided. The soil is a loam characterized by its texture and density which were determined in the laboratory. The w_{wilt} and the field capacity parameters were derived from the clay content observations, by using the relationships given by Noilhan and Mahfouf (1996).

2.2. Land surface model: ISBA-A-g_s

The land surface model used in this study is the ISBA-A-g_s model (Calvet et al., 1998, Calvet et al., 2004, Gibelin et al., 2006). It is an improved version of the Interaction between the Soil, Biosphere and Atmosphere (ISBA) model, first developed by Noilhan and Planton

(1989) and further improved by Noilhan and Mahfouf (1996), to describe the land surface processes in weather and climate models.

The version of the ISBA model used in this study is based on the equations of the force-restore method (Deardorff, 1977, 1978), and the soil is represented by a single layer. Together with the surface fluxes (*LE, H, G*), five surface state variables are described: surface temperature (T_s), mean surface temperature (T_2), surface volumetric soil moisture (w_g), volumetric root-zone soil moisture (w_2) and canopy interception reservoir (W_s). The new version (ISBA-A-g_s) accounts for the effect of the atmospheric CO_2 concentration on the stomatal aperture. The net assimilation of CO_2 is used to predict the vegetation biomass and the *LAI*. The model simulates two above-ground biomass reservoirs: the leaf biomass and the above-ground structural biomass. For herbaceous vegetation, the sum of these two reservoirs is the total above-ground biomass (*Bio*). The reservoirs are fed by the net assimilated carbon, and decreased by turnover and respiration terms. Phenology is modelled implicitly: LAI follows the variations of the leaf biomass, multiplied by a constant Specific Leaf Area (SLA). The SLA is related to the leaf nitrogen concentration (N_l) by using two plasticity parameters *e* and *f* (Gibelin et al. 2006):

$$SLA = eN_l + f \ . \qquad [1]$$

The values of *e* and *f* used in this study are presented in Table 1.

Two strategies are represented for the response of the plant to water stress, drought-avoiding and drought-tolerant (Calvet 2000, Calvet et al. 2004) depending on the evolution of water use efficiency (WUE) under moderate stress: WUE increases in the early stages of soil water stress in the case of the drought-avoiding response, whereas WUE decreases or remains stable in the case of the drought-tolerant response.

The vegetation parameters of ISBA-A-g_s are presented in Table 1. They are derived from the simulation of Calvet (2000) for the MUREX test site (Calvet et al., 1999). Following their work, the drought-tolerant strategy is used in this paper.

In this study, the model performance is evaluated by using the root mean square error (RMSE), the mean bias, and the efficiency score (or Nash criterion ; Nash and Sutcliffe 1970) E defined as:

$$E = 1 - \frac{\sum_i (x_i^{OBS} - x_i^{simulated})^2}{\sum_i (x_i^{OBS} - \overline{x^{OBS}})^2} \qquad [2]$$

where x represents a state variable and x^{OBS} the corresponding observed variable. A value of E equal to 1 corresponds to perfect simulations and values of E close to 0 correspond to simulations equal to the constant average of the observations. Negative values of E show that the model performance is less accurate than simply applying the arithmetic mean of the observations.

2.3. Assimilation method: Simplified 1D-VAR

The choice of the assimilation scheme is based on the results obtained in MU07. Of the four assimilation methods compared in that study, the Ensemble Kalman Filter (EnKF) and a simplified 1D-VAR showed the best performance. However, the variational scheme presented an important advantage, as the computational cost was significantly lower, making it more suitable for operational purposes. Therefore, a simplified 1D-VAR was employed in this study.

2.3.1. Formalism

Variational methods use an assimilation window of predefined length, usually containing several observations. The initial value of the model state vector (the variables to be analysed) is perturbed and the optimal combination of model states is then found by

minimizing a cost function J (at observation times within the assimilation window). In our case, the state vector is composed of two state variables (w_2 and vegetation above-ground biomass (Bio)). The cost functions for the two state variables are:

$$J(Bio) = \frac{1}{2}\left(Bio - Bio^{b}\right)^{T}\mathbf{B}_{BIO}^{-1}\left(Bio - Bio^{b}\right) + \frac{1}{2}\left(LAI^{OBS} - H(Bio)\right)^{T}\mathbf{R}_{LAI}^{-1}\left(LAI^{OBS} - H(Bio)\right) = J_{Bio}^{b} + J_{LAI}^{OBS} \quad [3]$$

$$J(w_g) = \frac{1}{2}\left(w_2 - w_2^{b}\right)^{T}\mathbf{B}_{w2}^{-1}\left(w_2 - w_2^{b}\right) + \frac{1}{2}\left(w_g^{OBS} - H(w_2)\right)^{T}\mathbf{R}_{wg}^{-1}\left(w_g^{OBS} - H(w_2)\right) = J_{w2}^{b} + J_{wg}^{OBS} \quad [4]$$

where the superscripts ^{b} and ^{OBS} denote the initially estimated values of the state variables within the assimilation window (background) and the observed variables, respectively; and H is the non-linear observation operator which transfers the state variables into observation space. The "best" analyses are the result of minimizing the distance between the state variables and the first-guess weighted by the background error covariance matrix $\mathbf{B}$ (J_{Bio}^{b} and J_{w2}^{b} terms) and the distance between the observations and the model predictions (J_{LAI}^{OBS} and J_{wg}^{OBS} terms) within the assimilation window, weighted by the observation error covariance matrix $\mathbf{R}$. In the case of a linear observation operator and a normal distribution of the errors, the analysed state variables of the cost functions [3] and [4] are expressed by :

$$Bio = Bio^{b} + \mathbf{K}_{BIO}\left(LAI^{OBS} - \mathbf{H}_{BIO}\left(Bio^{b}\right)\right); \quad \mathbf{K}_{BIO} = \mathbf{B}_{BIO}\mathbf{H}_{BIO}^{T}[\mathbf{H}_{BIO}\mathbf{B}_{BIO}\mathbf{H}_{BIO}^{T} + \mathbf{R}_{LAI}]^{-1}, \quad [5]$$

and

$$w_2 = w_2^{b} + \mathbf{K}_{w2}\left(w_g^{OBS} - \mathbf{H}_{w2}\left(w_2^{b}\right)\right); \qquad \mathbf{K}_{w2} = \mathbf{B}_{w2}\mathbf{H}_{w2}^{T}[\mathbf{H}_{w2}\mathbf{B}_{w2}\mathbf{H}_{w2}^{T} + \mathbf{R}_{wg}]^{-1}, \qquad [6]$$

respectively. In the non-linear case, the minimum of the cost functions [3] and [4] is evaluated by deriving adjoint or tangent linear models. However, this is an often difficult and time consuming task (Reichle et al., 2002). The simplified 1D-VAR (Balsamo et al., 2004) circumvents this problem by using a numerical linear approximation of the observation

operator. This approximation consists of a perturbation of the initial value of the state variables ($w_2 = w_2^b + \delta w_2$ for the root zone soil moisture and $Bio^{'} = Bio^{b} + \delta Bio$ for the vegetation biomass) and studying the impact of this perturbation on the predicted variables at each observation time step *i* within the assimilation window (with n observations). In this way, linearised observation operators of the type: $\mathbf{H} = \left[\frac{\delta y^1}{\delta x^0}, ..., \frac{\delta y^n}{\delta x^0} \right]$ are obtained, where $\delta \mathbf{x}^0$ represents the perturbation of the initial state variable and $\delta \mathbf{y}^i$ the change in the simulated variable at time step i (for i=[1,n]), due to $\delta \mathbf{x}^0$. This operator $\mathbf{H}$ is then substituted in [5] and [6], and also replaces the non-linear observation operator *H*.

2.3.2. Setting of the main 1D-VAR parameters

The most difficult task in the implementation of an assimilation scheme is the description of the error matrices. It is a key aspect, because the correction of the system state depends on the background and observation error prescription (see Eqs. [3] to [6]). The size of the initial perturbation and the length of the assimilation window is also discussed in this section.

(i) Assimilation window length

The choice of the assimilation window length for a variational assimilation scheme is particularly important when the scheme is applied to large regions. In this study, a 10-day assimilation window, which is close to the sampling time of many LAI products (e.g. a 8-day MODIS product is available), was chosen because shorter assimilation windows would regularly exclude LAI observations altogether.

(ii) Observational errors

In this study, observed time series of surface soil moisture (w_g) and LAI were used for the assimilation into the model. For w_g, the same method as in MU07 was applied, i.e. the error derived from the dispersion of in-situ observations was doubled and therefore set to $\mathbf{R}_{wg}$

= 0.06 m^3m^{-3}. For LAI, an observational error is difficult to obtain from the experimental procedure followed in SMOSREX. Moreover, the LAI observations exhibited quite different cycles (in terms of shape and maxima) in 2001 and 2002. It was decided to use an empirical value of $\mathbf{R}_{LAI}$ = 1 m^2m^{-2}, which is expected to account for all sources of uncertainties (observational system and representativeness error). Both values were assumed to be constant throughout the whole period 2001-2004. A sensitivity study was performed in order to assess the value of a variable LAI observation error. However, no or little impact on the assimilation results were found. For the sake of simplicity, a constant value was used.

(iii) Background errors

For the description of the error in the estimation of w_2, an ensemble of simulations was created between two consecutive observations by using different initial states of w_2 and by perturbing the atmospheric forcing. For each assimilation window the dispersion of the residuals (difference between an observation and the model estimation) was assessed. During the calibration year (2001) this quantity was shown to have a constant value of 0.02 m^3m^{-3}. The same approach was used to estimate a model covariance error for the vegetation biomass over the 10-days of the individual assimilation windows. It was observed that the evolution of the standard deviation of the residuals does not vary much over the year 2001. However, a slight seasonal effect is observed (not shown). Departure from the mean value is about 0.01 kg m^{-2} on average. Therefore, the background error for the vegetation biomass was assumed to be constant and was set equal to the average of the standard deviation of the residuals in 2001 (0.05 kg m^{-2}).

(iv) Linear hypothesis

A further important parameter in the implementation of this simplified variational assimilation scheme is the choice of the perturbation size of the state variables, because it determines the quality of the linear approximation through the observation operator **H**. To

evaluate the "optimal" size of this perturbation, the following test was conducted: an ensemble of linear operators **H** was obtained by finite differences (by a random Gaussian perturbation of the initial value of w_2 and/or the vegetation biomass) for a 10-day period (four components for $\mathbf{H}_{w2}$ and one for $\mathbf{H}_{BIO}$) and their standard deviation (σ) was calculated. Several values of the initial perturbation of the state variables were tested. The smallest perturbations of w_2 (between 0.005 and 0.015 m^3m^{-3}) produced a strong value of σ to the four linearized components of $\mathbf{H}_{w2}$ during the calibration year (not shown). This is due to the numerical noise produced by infinitesimal perturbations in the vicinity of the initial value. The most suitable perturbation should result in a low sensitivity of $\mathbf{H}_{w2}$. $\mathbf{H}_{w2}$ was found to be less sensitive for perturbations close to 0.05 m^3m^{-3} and this value was used in the assimilation algorithm.

Fig. 2 illustrates how the optimal perturbation of *Bio* was determined. The σ of the sole component of $\mathbf{H}_{BIO}$ in a 10-day assimilation window is presented for contrasting values of perturbations of *Bio*. In Fig. 2, the optimal perturbation, producing the lowest σ values, is located between 0.07 and 0.10 kg m^{-2}. It was finally set to 0.07 kg m^{-2}. Fig. 2 shows that perturbation values lower than 0.07 kg m^{-2} and between 0.10 and 0.13 kg m^{-2} produced larger σ values. Perturbations higher than 0.13 kg m^{-2} were found also to produce larger uncertainties in $\mathbf{H}_{BIO}$ (not shown).

(v) Implementation

The implementation of the simplified assimilation scheme can be undertaken in different ways. In this study, w_2 and vegetation biomass were perturbed at the beginning of each assimilation window, in order to determine the linearized observation operator. This configuration necessitated 3 runs for each assimilation window (one for each perturbed variable and one for the control run).

2.3.3. Dynamical correction of the wilting point

As mentioned before, w_{wilt} is estimated by the LSM and then treated as a constant parameter (found to be 0.17 m^3m^{-3} for the SMOSREX site). However, the assimilation scheme is allowed to initialise the model with w_2 states below w_{wilt}, following the assimilation of w_g. This occurred during the drought periods of the years 2003 and 2004 (MU07). In this case, ISBA-A-g_s did not allow any further evapotranspiration and soil water extraction through the roots, even after significant rainfall events. This led to a strong vegetation mortality rate. However, the SMOSREX field observations performed during the summer 2003 show that the vegetation growth in response to rainfall may be rapid (Fig. 1). The performance of the vegetation analyses was also affected by this constraint. The following solution is proposed: for each assimilation step with an analysed value of w_2 below the fixed w_{wilt}, the model w_{wilt} is re-set by substituting its value with the analysed value of w_2. This simple modification to the model allows plant growth in response to rainfall to occur after a drought.

3. Results

3.1. w_2 and biomass analyses (2001-2004)

In Fig. 3, the 1D-VAR analysis of w_2 and the vegetation biomass are presented for the years 2001 to 2004 (Fig. 3a and 3b, respectively) with a non-stationary w_{wilt} (see section 2.3.3). The simulation performed with ISBA-A-gs and without the assimilation of w_g or LAI observations (i.e. the control simulation) is also presented in Fig. 3. The predicted LAI (control and analysis) is also shown on Fig. 3c. The assimilated observations are the surface soil moisture (one observation every three days) and the LAI (one observation every 10 days). Analyses, observations and the control model reference are superposed for comparison purposes. It is shown that w_2 is generally well reproduced during the whole period from 2001 to 2004, with a score E equal to 0.86 after the assimilation in contrast to 0.79 for the control simulation (Table 2). The added value of the assimilation is particularly noticeable during the six months following June 2003, for which the model without assimilation is not able to descend below the prescribed w_{wilt} and consequently overestimates the moisture during the rest of that year.

On Fig. 3c, the impact of the joint w_2 and vegetation biomass analysis is shown for the LAI predictions. The predicted values of LAI are quite close to the observations, improving the performance from E = 0.17 for the control run to E = 0.72, and RMSE from 0.80 $m^2 m^{-2}$ to 0.47 $m^2 m^{-2}$ after the assimilation (Table 2). The main disagreements are found during the senescence periods of the vegetation when the model clearly overestimates the LAI (except for 2003, where an anomalous double cycle of LAI was observed). Since the vegetation biomass observations are sparse and very scattered for 2001 and 2002, it is not clear whether the assimilation improves the control model simulation for these years. It is observed that during the second cycle of vegetation in 2003, the biomass is slightly overestimated after the

analysis, which is in agreement with the higher LAI observations assimilated. The RMSE and the score for the years 2003 and 2004 were not improved, which may be explained by the limited number of available observations of vegetation biomass. However, for the whole study period, the analysis of the vegetation biomass improved the score from 0.17 to 0.23.

In Fig. 4, the impact of setting a non-stationary w_{wilt} is only shown for 2003 and 2004, because w_{wilt} was only modified during these two years. During the periods with analysed w_2 below w_{wilt} an increased vegetation mortality rate is observed. The need for re-setting w_{wilt} is particularly apparent between July and October 2004, when the vegetation biomass analyses were close to zero. During this period, each time w_2 analyses were below w_{wilt} ISBA-A-g_s stopped plant transpiration and photosynthesis, which resulted in a high vegetation mortality rate. Consequently, the performance of the vegetation biomass analyses for 2003 and 2004 was low (Table 2) compared to the case of a modified w_{wilt}. This effect is less evident in 2003, since the drying period is shorter than in 2004. For the complete four years, the score of the vegetation biomass decreases (compared with a non-stationary w_{wilt}) from 0.23 to 0.12. The lower vegetation biomass during the dry periods also had an impact on the soil water reservoir, which produced higher moisture levels. The score for w_2 decreased from 0.86 to 0.82 (Table 2).

3.2. Zero precipitation

The simulations at SMOSREX are forced with good quality measurements of meteorological variables, representative for the study area. However, at larger scales the information about meteorological variables is less accurate. In order to test the robustness of the 1D-VAR, even when forcing data are subjected to large errors, the precipitation was set to 0. Precipitation is a key variable within atmospheric forcing data sets and is particularly important for the water reservoir evolution. For this experiment, the assimilation scheme was run again for the whole 4-year period under investigation. Fig. 5 shows the same plots as Fig. 3, but with the new, degraded forcing data. Although the new analyses produced a drier soil, the general shape of the curve of the analyzed w_2 was maintained. It is now much smoother, since the information about the precipitation events is lacking. It is important to remark that the assimilation scheme permits the increase of the root-zone soil moisture before the start of the growing period. Otherwise, given the absence of precipitation, a growing season would not be simulated. The LSM, with precipitation set to 0, tends to decrease the root-zone soil moisture between two observations. However, the 1D-VAR generates positive increments which correct the water deficiency in order to match the w_g observations. The advantage over the control simulation is considerable. Under the precipitation constriction, the control simulation would rapidly fall to 0.17 m^3m^{-3} (constant w_{wilt}), and since the model would not receive precipitation, the moisture reservoir would remain at this lower boundary. The benefits of the data assimilation are also clear for the vegetation: although the biomass analyses are obtained with less accuracy (in particular, lower peak values are obtained), especially during the wet years 2001 and 2002, the start of the growing season is still well predicted. The need for a non-stationary w_{wilt} is highlighted again when Fig. 5 is compared to

Fig. 6. In the latter, the vegetation biomass reaches a value of 0 in those periods where w_2 is below w_{wilt}, and which now have a longer duration, due to the lack of precipitation. The score for the vegetation biomass becomes negative and for the LAI is reduced from 0.48 (non-stationary w_{wilt}) to 0.14 (stationary w_{wilt}). In Fig. 6, the w_2 analyses for the summer period are overestimated in the years 2003 and 2004, because of a very low level of vegetation, while better retrievals are obtained by re-setting w_{wilt}. The evapotranspiration is strongly reduced without precipitation, since the simulation of the vegetation biomass underestimates the real conditions (Table 3).

4. Summary and Discussion

The present study is a continuation of the work initiated in MU07. There, a simplified 1D-VAR assimilation scheme was compared with other assimilation schemes, and it was shown that it offered the best performance in view of a future implementation in a regional experiment. However, the LAI was forced and the vegetation biomass was not corrected for, as only w_g observations were assimilated. Nevertheless, vegetation biomass is also an important surface variable, vital to estimate the carbon and water vapour fluxes, and its analysis is also essential. In this study, field observations of w_g and LAI were assimilated at the same time into the ISBA-A-g_s LSM. When comparing Fig. 3a of this study with Fig. 4 of MU07, two main differences are observed with regard to the analyses of w_2: i) a degradation at the end of 2001 is observed, ii) the correction over the dry period of 2004 is less accurate. This is a consequence of analysing the vegetation biomass in addition to soil moisture. From October 2001 to February 2002 no LAI observations were available, which resulted in interpolated values of less than 0.5 m^2m^{-2} during this period. In this study, these estimates were assimilated and the LAI retrievals after assimilation were close to these observations. This produced lower transpiration and water extraction rates, hence a slower drying of the

water reservoir and as a consequence an overestimation of the w_2 analyses. Before the implementation of the joint assimilation of w_g and LAI observations into the fully coupled model, a number of tests were performed. In particular, the assimilation of w_g alone and of LAI alone was attempted (MU07).

The assimilation of w_g alone (LAI was not controlled by any observation) did not improve the simulated LAI. It tended to speed up the growing period and to increase the maximum value of LAI reached each year. This factor had detrimental effects on the analysed w_2 during the spring of 2002 (values lower than the control simulation, and much lower than the observations were obtained).

The assimilation of LAI alone (w_g was not constrained by any observation) generally improved w_2 only marginally. However, it tended to increase the error on the simulated w_2 during the drought periods (e.g. October 2001, July-August 2003, July 2004, October 2004), while it permitted to obtain analysed vegetation biomass values very similar to those shown in Figs. 3 and 4.

No flux validation data was available and the positive or negative impact of the assimilation on the fluxes could not be quantified. On a daily basis, the simulated evapotranspiration was not fundamentally changed by the assimilation. However, the new annual cycles of the flux was more consistent with the available observations of vegetation biomass and LAI, which showed that the LAI produced by the control simulation was underestimated during the start of the growing season and overestimated during the senescence phase.

The w_{wilt} limitation imposed by the single soil layer of the model used in this study tends to trigger a high vegetation mortality rate during marked droughts, and to underestimate the impact (on vegetation growth and on the water and carbon fluxes) of significant rainfall events after the droughts. A simple solution consists in re-setting w_{wilt} dynamically during

anomalously dry periods. The introduction of a non-stationary w_{wilt} was shown to improve the moisture and vegetation predictions as compared to the control simulation with a stationary w_{wilt}. This led to an improvement of the score of w_2 from 0.79 to 0.86. Furthermore, the score was slightly improved from 0.17 to 0.23 for the vegetation biomass analysis. The final value of 0.23 is rather low, partly because the high level of scatter in the observations found for 2001 and 2002 prevents the score of reaching higher values.

Solutions potentially suitable to overcome the w_{wilt} problem, include the attribution of more weight to the LAI observations by reducing the observational error when the initial w_2 is found below the prescribed w_{wilt}. However, this poses a problem when LAI observations are not reliable. The simple solution of prescribing a non-stationary w_{wilt} value, low enough for drought periods, was assessed (not shown). Indeed, a lower w_{wilt} (e.g. 0.10 m^3m^{-3} instead of 0.17 m^3m^{-3}) permitted to improve the control simulation of w_2 during the summer/autumn of dry years (2003-2004). However, this change triggered a significant underestimation of w_2 during the summer/autumn of the normal/wet years (2001-2002). These results were to be expected, as prescribing a lower value of the wilting point is tantamount to increasing the total extractable soil moisture of the soil. The vegetation simulated by ISBA-A-gs over this site tends to exploit the whole soil moisture reservoir prescribed in the model, even during a wet year like 2002. It was eventually decided that it was preferable to use the 0.17 m^3m^{-3} value, which is a typical wilting point value for a loam and which allows a good model performance during normal years. The difference between the model and the observations in 2003 and 2004 can be explained by the rather extreme droughts encountered during these two years. A number of biological and physical explanations are proposed:

In the model, the wilting point depends on the soil texture. In reality, this parameter may also depend on the plant ability to extract water from a particular soil. The SMOSREX fallow is a multi-specific canopy. During drought events, the plant species most capable of extracting

water in dry conditions have an advantage in their competition with the other species. This effect could change the behaviour of the soil-plant system from one year to another. To some extent, this effect could also happen at large spatial scales for natural ecosystems and agricultural areas (e.g. farmer may choose to use cultivars adapted to dry conditions during dry years).

Over the SMOSREX site, the fallow biomass is very dense and the dead vegetation residues tend to form a dense vegetal mulch at the soil surface (De Rosnay et al. 2006). In the model, the strong decrease in direct soil evaporation due to the mulch (Gonzalez-Sosa et al. 2001) is not represented explicitly. In order to represent the mulch effect, a fixed vegetation cover fraction of 100 % was assumed in the ISBA-A-gs simulations. Test simulations were performed with lower vegetation cover fraction values (allowing bare soil evaporation) and showed that this effect is not sufficient to simulate a total soil moisture content below the wilting point. In the field, phenomena like the formation of deep cracks into the soil may foster the soil evaporation and this process is not accounted for by the model.

The use of a soil multi-layer scheme, which describes more accurately the evolution of the prognostic variables during dry periods than a single layer model with an averaged soil moisture content, may lead to a better prediction of soil moisture and LAI. In particular, the impact on the vegetation of rewetting the top soil layer is better accounted for by a multilayer model. However, the inclusion of several soil layers would augment the computational burden of the assimilation. The assimilation of observations into a multi-layer soil model is not a simple task. If all layers are to be analysed individually, an understanding of the error-correlation between near-surface soil moisture observations and the different layers are required (Reichle et al. 2001, Walker et al. 2002).

It was shown that when precipitation observations contain large errors, the joint assimilation of w_g and LAI is capable of restoring the annual trend of w_2 and vegetation

biomass, but large errors may occur in the absolute value of these quantities. An attempt was made to deactivate the plant growth module of the model and to analyse w_2 only. In this case, the observed LAI was prescribed to the model instead of being assimilated. The soil moisture evolution was better predicted, because the root-plant water extraction and evapotranspiration rates were more realistic. In case of large precipitation errors, imposing LAI from external observations may be an advantage for the retrieval of soil moisture. However, as stated above, a large error in the LAI observations may prevent the assimilation scheme to lead to a significant improvement.

In this study, an assimilation window of 10 days was used. Longer windows have the advantage of reducing the computing time but they result in a degradation of the model prediction. For example, a test with a 30-day assimilation window showed that the score E of the analysed w_2 and vegetation biomass decreased from 0.86 and 0.23, respectively, to 0.79 and a negative value.

5. Conclusion

In the SMOSREX case study, the joint assimilation of w_g and LAI observations by using a simplified 1D-VAR assimilation scheme over a fallow, has demonstrated that:

- The temporal evolution of both w_2 and the vegetation biomass are significantly improved by the assimilation. The assimilation scheme generally reduces the model underestimation of vegetation biomass during the growing phase and, especially, the overestimation of vegetation biomass during the senescence phase of the vegetation.
- The use of a non-stationary w_{wilt} is required for dry years during which soil moisture observations are found below the a priori value of w_{wilt}. This change limits

the vegetation mortality during (and after) very dry conditions and the underestimation of the evapotranspiration following an inaccurate simulation of the biomass.

- In the presence of significant errors in the atmospheric forcing, the leaf onset and the seasonal dynamics of the soil moisture are still retrieved well even, for example, if precipitation is set to 0. However, the error on the analysed variables (w_2 and the vegetation biomass) is large. In this case, the analysis of w_2 is more efficient if the vegetation biomass is not analysed, i.e. if good quality LAI observations are prescribed to the model, instead of simulating the vegetation growth.

Acknowledgements

This study was co-funded by the European Commission within the GMES initiative in FP6, in the framework of the GEOLAND integrated GMES project on land cover and vegetation. The SMOSREX experiment was co-funded by a TOSCA grant from CNES. The authors would like to thank Dr. Gianpaolo Balsamo (ECMWF, Reading) for fruitful discussions, as well as the anonymous reviewers, for their helpful comments.

References

Balsamo, G., Bouyssel, F., Noilhan, J., 2004. A simplified bi-dimensional variational analysis of soil moisture from screen-level observations in a mesoscale numerical weather-prediction model. *Q. J. R. Met. Soc*., **130A**, 895-915.

Bicheron, P., Leroy, M., 1999. A method of biophysical parameter retrieval at global scale by inversion of a vegetation reflectance model. *Remote Sens. Environ*., **67**, 251-266.

Bounoua, G. J., Collartz, G. J., Los, S. O., Sellers, P. J., Dazlich, D. A., Tucker, C. J., Randall, D., 2000. Sensitivity of climate to changes in NDVI. *J. Clim*., **13**, 2277-2292.

Calvet, J.-C., Noilhan, J., Roujean, J.-L., Bessemoulin, P., Cabelguenne, M., Olioso, A., Wigneron, J.-P., 1998. An interactive vegetation SVAT model tested against data from six contrasting sites. *Agric. For. Meteor*., **92**, 73-95.

Calvet, J.-C., Bessemoulin, P. Noilhan, J., Berne, C., Braud, I., et al., 1999. MUREX: A land-surface field experiment to study the annual cycle of the energy and water budgets. *Ann. Geophys*., **17**, 838-854.

Calvet, J.-C., 2000. Investigating soil and atmospheric plant water stress using physiological and micrometeorological data. *Agric. For. Meteor*., **103**, 229-247.

Calvet, J.-C., Soussana, J.F., 2001. Modelling CO_2 enrichment effects using an interactive vegetation SVAT scheme. *Agric. For. Meteor*., **108**, 129-152.

Calvet, J.-C., Rivalland, V., Picon-Cochard, C., Guehl, J.-M., 2004. Modelling forest transpiration and CO_2 fluxes - response to soil moisture stress, *Agric. For. Meteorol.,* **124**(3-4), 143-156, doi: 10.1016/j.agrformet.2004.01.007.

Cayrol, P. , Chehbouni, A., Kergoat, L., Dedieu, G., Mordelet, P., Nouvellon, Y., 2000. Grassland modeling and monitoring with SPOT-4 VEGETATION instrument during the 1997-1999 SALSA experiment, *Agric. For. Meteorol*., **105**, 91-115.

Chase, T. N., Pielke, R. A., Kittel, T. G. F., Nemani, R., Running, S. W., 1996. The sensitivity of a general circulation model to global changes in leaf area index. *J. Geophys. Res.*, **101**, 7393-7408.

De Rosnay, P., Calvet, J.-C., Kerr, Y., Wigneron, J.-P., Lemaître, F., Escorihuela, M.J., Muñoz Sabater, J., Saleh, K., Barrie, J., Coret, L., Cherel, G., Dedieu G., Durbe, R.., Fritz, N.E.D., Froissard, F., Kruszewski, A., Lavenu, F., Suquia, D., Waldteufel, P., 2006. SMOSREX: A long term field campaign experiment for soil moisture and land surface processes remote sensing. *Remote Sens. Environ*., **102**, 377-389.

Deardorff, J. W., 1977. A parameterization of ground-surface moisture content for use in atmospheric prediction models. *J. Appl. Meteor.*, **16**, 1182-1185.

Deardorff, J. W., 1978. Efficient prediction of ground surface temperature and moisture with inclusion of a layer of vegetation. *J. Geophys. Res*., **20**, 1889-1903.

Entekhabi, D., Nakamura, H., Njoku, E.G., 1994. Solving the inverse problem for soil moisture and temperature profiles by sequential assimilation of multifrequency remotely sensed observations. *IEEE Trans. Geos. Remot. Sens*., **32**(2), 438-448.

Gibelin, A.-L., Calvet, J.-C., Roujean, J.-L., Jarlan, L., Los S., 2006. Ability of the land surface model ISBA-A-g_s to simulate leaf area index at the global scale: comparison with satellites products, *J. Geophys. Res*., **111**, D18102, doi:10.1029/2005JD006691.

Gonzalez-Sosa, E., Braud, I., Thony, J.-L., Vauclin, M., Calvet, J.-C., 2001. Heat and water exchanges of fallow land covered with plant-residue mulch layer: a modeling study using the three year MUREX data set, *J. Hydrol*., **244**, 119-136.

Henderson-Sellers, A., Yang, Z.-L., Dickinson, R. E., 1993. The Project for Intercomparison of Land-surface Parameterization Schemes. *Bull. Am. Meteorol. Soc*., **74**, 1335-1349.

Henderson-Sellers, A., Pitman, A. J., Love, P. K., Irannejad, P., Chen, T. H., 1995. The Project for Intercomparison of Land-surface Parameterization Schemes (PILPS): Phases 2 and 3. *Bull. Am. Meteorol. Soc*., **76**, 489-503.

Houser, P.R., Shuttleworth, W.J., Famiglietti, J.S., Gupta, H.V., Syed, K.H., and D.C. Goodrich (1998). Integration of soil moisture remote sensing and hydrologic modeling using data assimilation, *Water Resour. Res.*, **34**, 3405-3420.

International GEWEX Project Office., 1995. Global Soil Wetness Project, version 1.0. 47 pp. [Available from International GEWEX Project Office, 1100 Wayne Avenue, Suite 1210, Silver Spring, MD 20910.].

Kerr, Y.H., Waldteufel, P., Wigneron, J.-P., Martinuzzi, J., Font, J., Berger, M., 2001. Soil moisture retrieval from space: the Soil Moisture and Ocean Salinity (SMOS) mission. *IEEE Trans. Geos. Remot. Sens*., **39**, 1729-1735.

Lakshmi, V. and J. Susskind (2001). Utilization of satellite data in land surface hydrology: sensitivity and assimilation. *Hydrol. Process.*, **15**, 877-892.

Muñoz Sabater, J., 2007. Assimilation de données de télédétection pour le suivi des surfaces continentales : mise en œuvre sur un site expérimental. PhD Thesis, University Toulouse III, Toulouse, 164 pp."

Muñoz Sabater, J., Jarlan, L., Calvet, J.-C., Bouyssel, F., De Rosnay, P., 2007. From near surface to root zone soil moisture using different assimilation techniques. *J. Hydrometeor.*, **8**, 194-206, doi: 10.1175/JHM571.1.

Nash, J. E., Sutcliffe, J. V., 1970. River flow forecasting through conceptual models, discussion and principles. *J. Hydrol*., **10**, 282– 290.

Njoku, E.G., Jackson, T.J., Lakshmi, V., Chan, T.K., Nghiem, S.V., 2003. Soil moisture retrieval from AMSR-E. *IEEE Trans. Geosc. Remote Sens*., **41**(2), 215 – 229.

Noilhan, J., Planton, S., 1989. A simple parameterization of land surface processes for meteorological models. *Mon. Wea. Rev.*, **117**, 536-549.

Noilhan, J., Mahfouf, J.-F., 1996. The ISBA land surface parameterisation scheme. *Global Planet. Changes*, **13**, 145-159.

Reichle, R. H., McLaughlin, D. B., Entekhabi, D., 2001. Variational data assimilation of microwave radiobrightness observations for land surface hydrology applications. *IEEE Trans. Geosci. Remote Sens*., **39**, 1708-1718.

Reichle, R.H., Walker, J.P., Koster, R.D., and P.R. Houser, 2002. Extended versus Ensemble Kalman Filtering for land data assimilation. *J. Hydromet.*, **3**, 728-740.

Roujean, J.-L., Lacaze, R., 2002. Global mapping of vegetation parameters from POLDER multiangular measurements for studies of surface-atmosphere interactions: a pragmatic method and validation. *J. Geophys. Res*., **107**, 4150.

Segal, M., Arritt, R. W., Clark, C., Rabin, R., Brown, J., 1995. Scaling evaluation of the effect of surface characteristics on potential for deep convection over uniform terrain. *Mon. Weather Rev*., **123**, 383-400.

Seuffert, G., Gross, P., Simmer, C., Wood, E.F., 2002. The influence of hydrologic modelling on the predicted local weather: Two-way coupling of a mesoscale weather prediction model and a land surface hydrologic model. *J. Hydrometeor*., **3**, 505-523.

Shaw, B. L., Pielke, R. A., Ziegler, C. L., 1997. A three-dimensional numerical simulation of a Great Plains dryline. *Mon. Weather Rev*., **125**, 1489-1506.

Tian, Y., Woodcock, C. E., Wang, Y., Privette, J. L., Shabanov, N. V., Zhou, L., Buermann, W., Dong, J., Veikkanen, B., Hame, T., Ozdogan M., Knyazikhin Y., Myneni, R. B., 2002a. Multiscale Analysis and Validation of the MODIS LAI Product I. Uncertainty assessment. *Remote Sens. Environ*. **83**, 414-430.

Tian, Y., Woodcock, C. E., Wang, Y., Privette, J. L., Shabanov, N. V., Zhou, L., Buermann, W., Dong, J., Veikkanen, B., Hame, T., Ozdogan M., Knyazikhin Y., Myneni, R. B., 2002b. Multiscale Analysis and Validation of the MODIS LAI Product II. Sampling strategy. *Remote Sens. Environ*. **83**, 431-441.

Tan, B., Hu, J., Huang, D., Yang, W., Zhang, P., Shabanov, N. V., Knyazikhin, Y., Nemani, R. R., Myneni, R. B., 2005. Assessment of the broadleaf crops leaf area index product from the Terra MODIS instrument, *Agric. For. Meteor*., **135**, 124-134.

Walker, J. P., Willgoose, G. R., Kalma, J. D., 2002. Three-Dimensional Soil Moisture Profile Retrieval by Assimilation of Near-Surface Measurements: Simplified Kalman Filter Covariance Forecasting and Field Application. *Water Resour. Res.*, **38** (12), 1301, doi:10.1029/2002WR001545.

Wigneron, J.-P., Pellarin, T., Calvet, J. –C., de Rosnay, P., Saleh, K., Kerr, Y., 2005. L-MEB: A simple model at L-Band for the continental areas – application to the simulation of a half-degree resolution and global scale data set. *Radiative transfer models for microwave radiometry*, Matzler C., ed, Stevenage, UK: Institution of Electrical Engineers

List of figures

1. a) *LAI*, b) w_g, c) w_2 and d) monthly precipitation for 2001 to 2004 as measured over the SMOSREX site. On top the interpolated *LAI* (solid line) is superimposed to the observations (circles). Note that the spline function used for *LAI* interpolation changed from one year to another, depending on data quality and frequency. The w_g and w_2 simulations of ISBA-A-g_s (solid line) using the offensive strategy as response to water stress (drought tolerant) are superimposed to the observations (dots for w_g and stars for w_2).

2. Temporal evolution of the linearized $\mathbf{H}_{BIO}$ standard deviation. $\mathbf{H}_{BIO}$ is computed by an initial perturbation of the vegetation biomass. The standard deviation of $\mathbf{H}_{BIO}$ is presented for four different intervals for the initial perturbation of the vegetation biomass: [0.005, 0.030], [0.03, 0.07], [0.07, 0.10], [0.10, 0.13], in units of kg m^{-2}. $\mathbf{H}_{BIO}$ values are in units of m^{2} kg^{-1}.

3. Analysis of a) the root zone soil moisture (circles) and b) vegetation biomass, using the simplified 1D-VAR method and a dynamical correction of the wilting point for 2001 to 2004 over the SMOSREX experimental site. c) Observations and simulations of *LAI* before and after the assimilation. For comparison purposes, analysed values are superimposed over the in-situ observations (points) and the open loop-simulations(solid line).

4. Analysis of a) the root zone soil moisture (circles) and b) vegetation biomass, using the simplified 1D-VAR method and a fixed wilting point for 2003 to 2004 over the SMOSREX experimental site. c) *LAI* before and after the assimilation. For comparison purposes, analysed values are superimposed over the in-situ observations (points) and the model initial estimations (solid line).

5. Analysis of a) root zone soil moisture and, b) vegetation biomass, using the simplified 1D-VAR method for 2001 to 2004, with precipitation set to zero. c) LAI before and after the assimilation. Analysed values (circles) are superimposed over the in-situ observations (points) and the model basic estimations (solid line) for comparison purposes.

6. Same as Fig. 5, but using a fixed wilting point. The results for the years 2001 and 2002 are omitted as being similar as in Fig. 5.

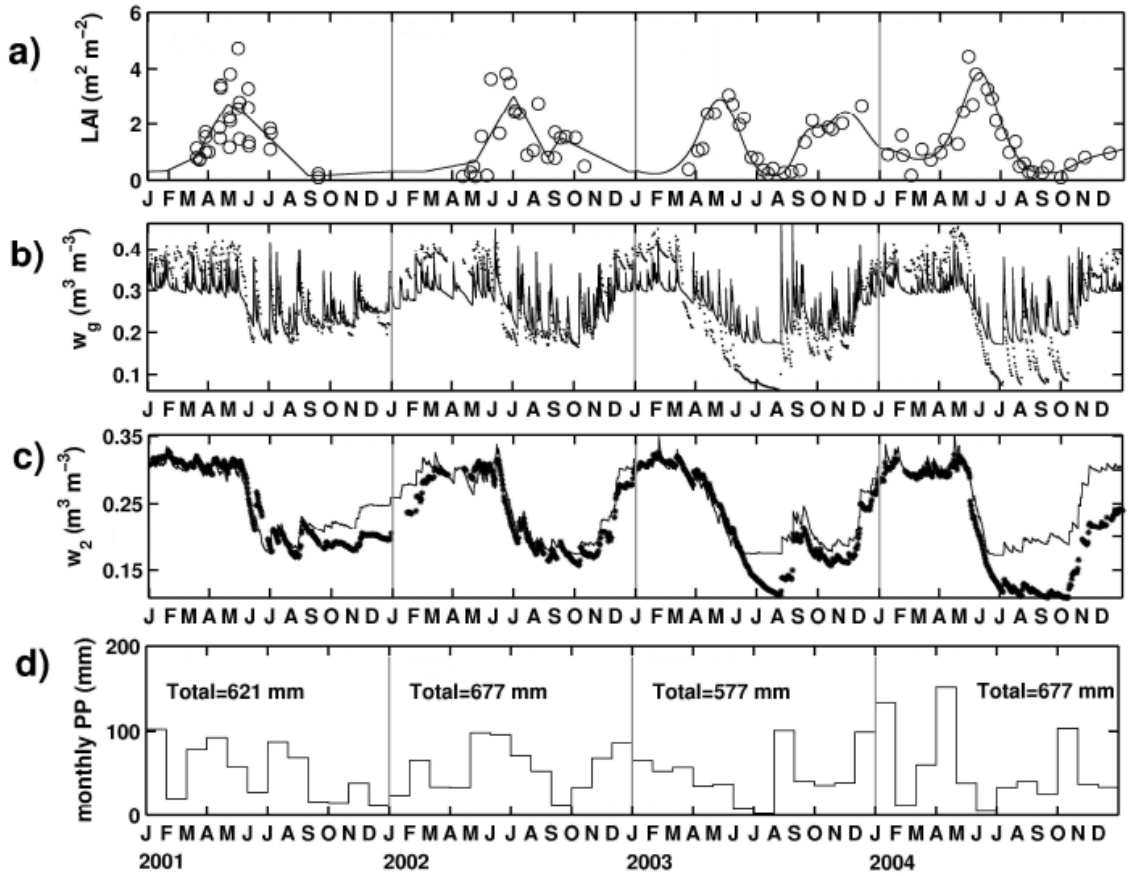

Figure 1.- a) *LAI*, b) w_g, c) w_2 and d) monthly precipitation for 2001 to 2004 as measured over the SMOSREX site. On top the interpolated *LAI* (solid line) is superimposed to the observations (circles). Note that the spline function used for *LAI* interpolation changed from one year to another, depending on data quality and frequency. The w_g and w_2 simulations of ISBA-A-g_s (solid line) using the offensive strategy as response to water stress (drought tolerant) are superimposed to the observations (dots for w_g and stars for w_2).

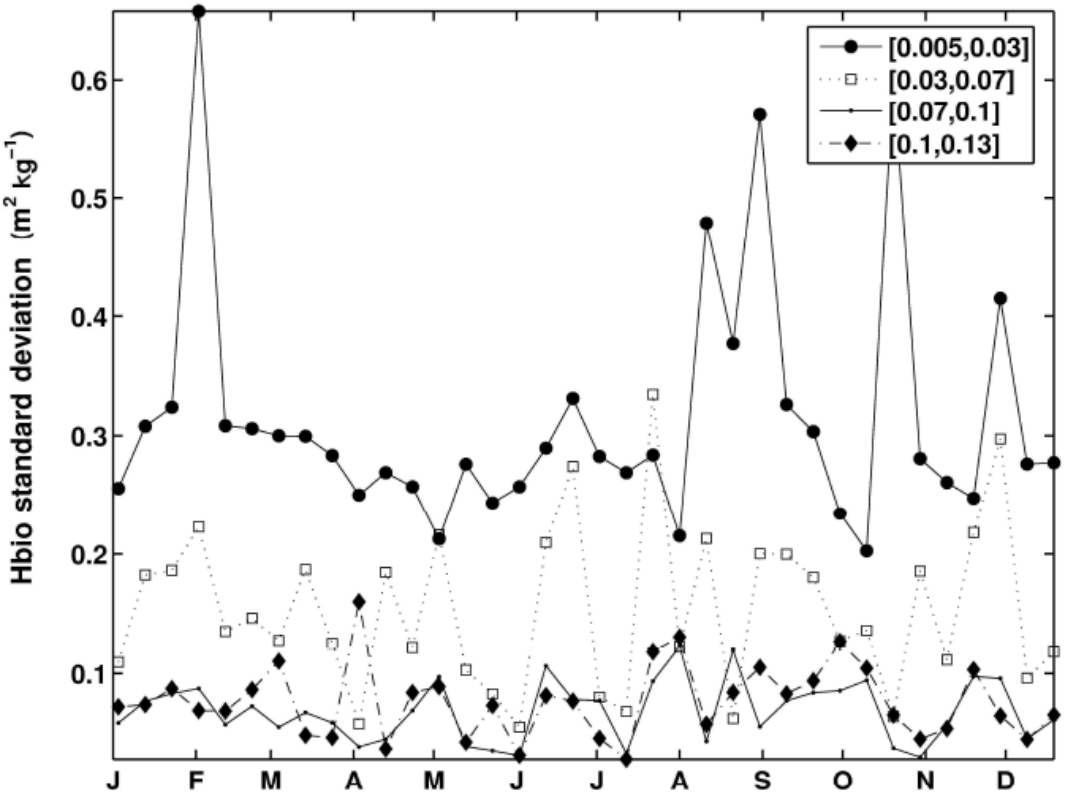

Figure 2.- Temporal evolution of the linearized $\mathbf{H}_{BIO}$ standard deviation. $\mathbf{H}_{BIO}$ is computed by an initial perturbation of the vegetation biomass. The standard deviation of $\mathbf{H}_{BIO}$ is presented for four different intervals for the initial perturbation of the vegetation biomass: [0.005, 0.030], [0.03, 0.07], [0.07, 0.10], [0.10, 0.13], in units of kg m^{-2}. $\mathbf{H}_{BIO}$ values are in units of m^{2} kg^{-1}.

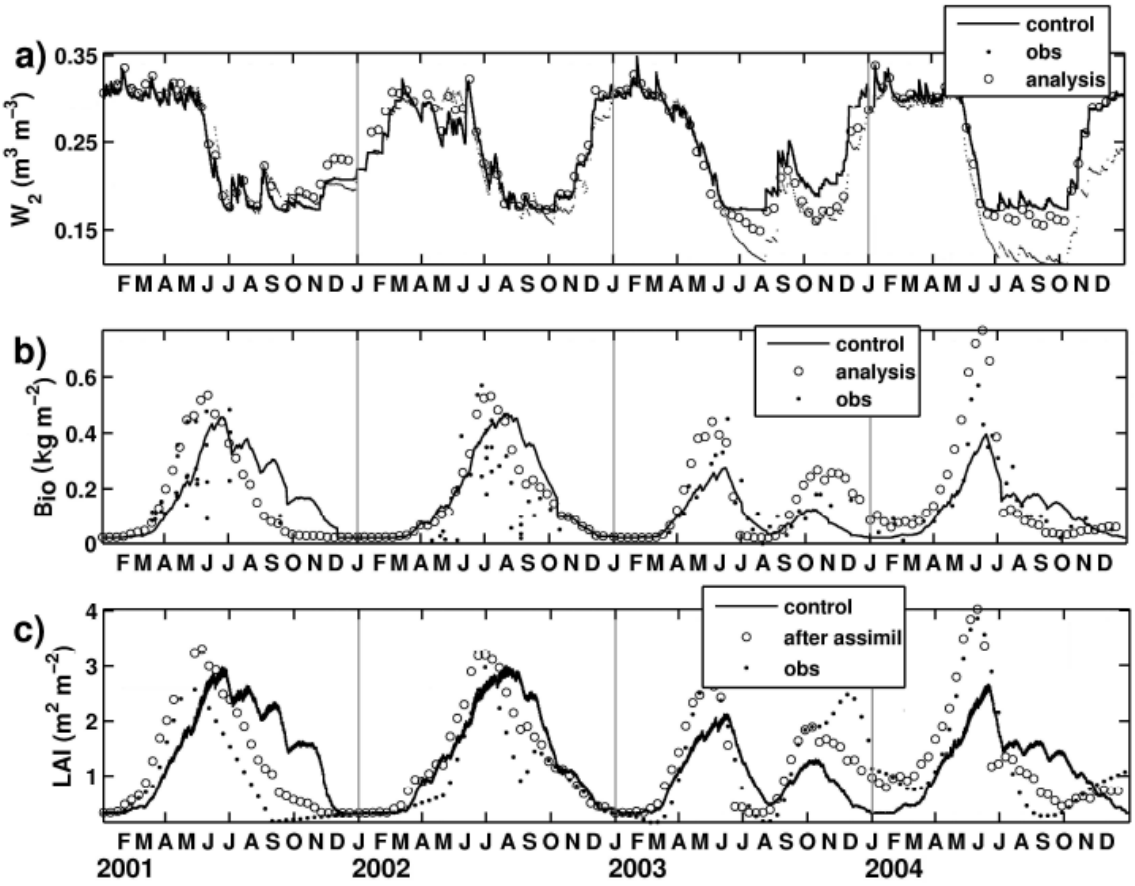

Figure 3.- Analysis of a) the root zone soil moisture (circles) and b) vegetation biomass, using the simplified 1D-VAR method and a dynamical correction of the wilting point for 2001 to 2004 over the SMOSREX experimental site. c) LAI before and after the assimilation. For comparison purposes, analysed values are superimposed over the in-situ observations (points) and the model basic estimations (solid line).

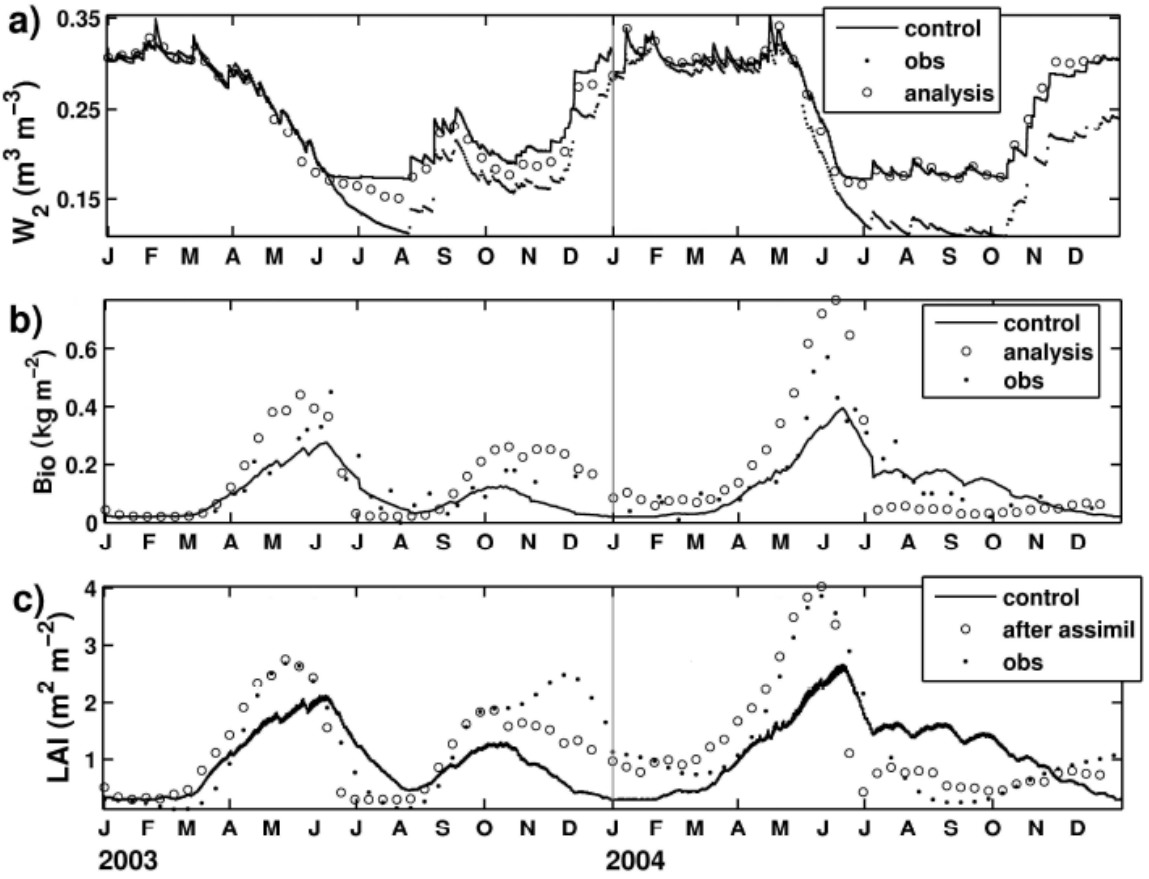

Figure 4.- Analysis of a) the root zone soil moisture (circles) and b) vegetation biomass, using the simplified 1D-VAR method and a fixed wilting point for 2003 to 2004 over the SMOSREX experimental site. c) *LAI* before and after the assimilation. For comparison purposes, analysed values are superimposed over the in-situ observations (points) and the model basic estimations (solid line).

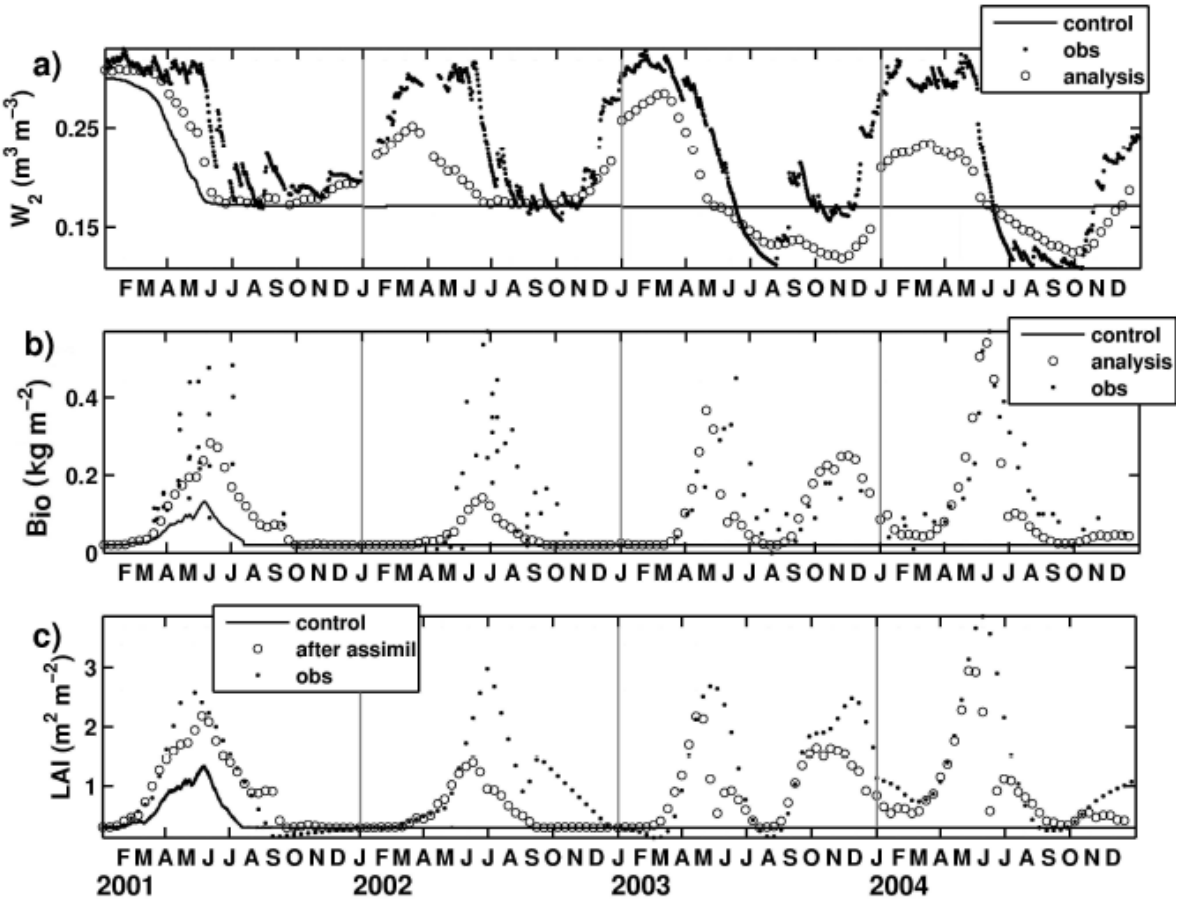

Figure 5.- Analysis of a) the root zone soil moisture and, b) vegetation biomass, using the simplified 1D-VAR method for 2001 to 2004, with precipitation set to zero. c) LAI before and after the assimilation. Analysed values (circles) are superimposed over the in-situ observations (points) and the model basic estimations (solid line) for comparison purposes.

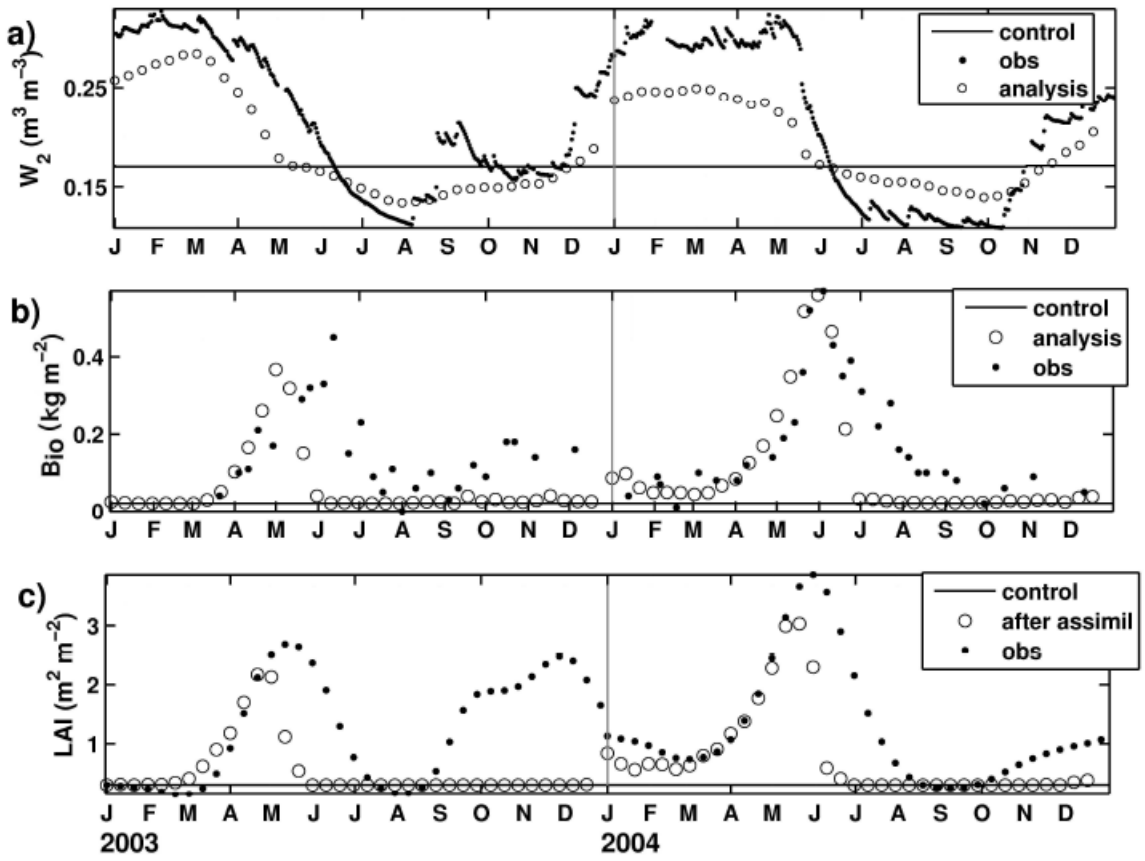

Figure 6.- Same as Fig. 5, but using a fixed wilting point. The results for the years 2001 and 2002 are omitted as being similar as in Fig. 5.

List of Tables

1.- Main soil and vegetation parameters used in the ISBA-A-g_s simulations over the SMOSREX site.

2.- Yearly and global RMSE (in $m^3\ m^{-3}$), mean bias (in $m^3\ m^{-3}$) and score (E) for the root zone-soil moisture, the above-ground vegetation biomass, and the LAI of the analyses (4 model configurations) and the control simulation.

3.- Evapotranspiration yearly cumulated flux (LE, in mm $year^{-1}$) after the assimilation of *LAI* and w_g observations for four different model configurations, and for the control simulation.

TABLE 1.

Main soil and vegetation parameters used in the ISBA-A-g_s simulations over the SMOSREX site.

Soil parameters			
parameter	**symbol**	**Unit**	**Value**
Soil depth	d_2	cm	95
Sand Content	SAND	%	32.0
Clay content	CLAY	%	22.8
Field capacity	w_{fc}	$m^3 \odot m^{-3}$	0.30
Wilting point	w_{wilt}	$m^3 \odot m^{-3}$	0.17
Vegetation parameters			
parameter	**symbol**	**Unit**	**Value**
Mesophyll conductance	g_m	$mm \odot s^{-1}$	0.56
Critical extractable soil moisture	θ_c	%	50
Plant response to water stress	-	-	drought-tolerant
Potential leaf life expectancy	τ	days	80
Minimum LAI	LAI_{min}	$m^2 \odot m^{-2}$	0.3
Cuticular conductance	g_c	$mm \odot s^{-1}$	0
Nitrogen plasticity parameter (slope)	e	$m^2 \odot kg^{-1} \odot \%^{-1}$	5.84
Nitrogen plasticity parameter (intercept)	f	$m^2 \odot kg^{-1}$	6.32
Leaf nitrogen concentration	N_l	%	1.4

TABLE 2.

Yearly and global RMSE and mean bias for the root zone-soil moisture (in $m^3 m^{-3}$), the above-ground vegetation biomass (in kg m^{-2}), and the LAI (in $m^2 m^{-2}$) of the analyses (4 model configurations) and the control simulation. The score E (dimensionless) is indicated.

		2001			2002			2003			2004			2001-2004		
		RMSE	mb	E	RMSE	mb	E	RMSE	mb	E	RMSE	mb	E	RMSE	mb	E
ANALYSIS Fixed w_{wilt}	w_2	0.01	0.03	0.94	0.02	0.01	0.90	0.02	0.01	0.90	0.05	0.04	0.60	0.03	0.01	0.82
	LAI	0.41	0.38	0.65	0.46	0.32	0.62	0.45	-0.07	0.75	0.50	-0.02	0.73	0.48	0.16	0.70
	Biomass	0.13	0.01	0.02	0.16	0.12	0.08	0.09	0.03	0.26	0.12	0.04	0.18	0.14	0.03	0.12
ANALYSIS Dynamic w_{wilt}	w_2	0.01	0.03	0.94	0.02	0.01	0.90	0.02	0.01	0.94	0.04	0.02	0.72	0.03	0.01	0.86
	LAI	0.41	0.38	0.65	0.46	0.32	0.62	0.41	-0.07	0.76	0.45	0.05	0.79	0.47	0.19	0.72
	Biomass	0.13	0.01	-0.21	0.16	0.12	-0.08	0.09	0.03	0.48	0.12	0.04	0.39	0.14	0.08	0.23
ANALYSIS PP=0, fixed w_{wilt}	w_2	0.03	-0.02	0.68	0.05	-0.04	-0.09	0.04	-0.03	0.65	0.05	-0.02	0.66	0.04	-0.03	0.57
	LAI	0.31	-0.02	0.81	0.73	-0.46	0.02	1.16	-0.72	-0.63	0.85	-0.49	0.27	0.82	-0.46	0.14
	Biomass	0.13	-0.07	0.03	0.18	-0.13	-0.38	0.15	-0.08	-0.94	0.11	-0.04	0.47	0.14	-0.08	-0.06
ANALYSIS PP=0, Dynamic w_{wilt}	w_2	0.03	-0.02	0.68	0.05	-0.04	-0.09	0.05	-0.04	-0.09	0.06	-0.03	0.51	0.05	-0.03	0.47
	LAI	0.30	-0.02	0.86	0.73	-0.46	0.02	0.73	-0.46	0.02	0.73	-0.36	0.46	0.64	-0.29	0.48
	Biomass	0.13	-0.07	0.03	0.18	-0.13	-0.38	0.10	0.03	0.15	0.09	-0.03	0.66	0.13	0.04	0.13
CONTROL	w_2	0.01	-.005	0.97	0.02	-.004	0.89	0.03	0.02	0.74	0.05	0.04	0.58	0.03	0.01	0.79
	LAI	0.97	0.47	-0.40	0.60	0.32	0.35	0.79	-0.33	0.25	0.81	-0.12	0.33	0.80	0.09	0.17
	Biomass	0.12	-.07	0.15	0.19	1.19	-.47	0.06	-0.03	0.53	0.08	-0.02	0.62	0.13	0.02	0.17

TABLE 3.

Evapotranspiration yearly cumulated flux (LE, in mm year^{-1}) after the assimilation of *LAI* and w_g observations for four different model configurations, and for the control simulation.

	2001	2002	2003	2004
Control	505.8	523.8	407.1	398.8
Analysis fixed w_{wilt}	535.8	520.5	378.5	375.4
Analysis dynamic w_{wilt}	543.8	520.4	400.0	395.2
Analysis fixed w_{wilt} and no rain	230.8	144.7	113.4	156.0
Analysis dynamic w_{wilt} and no rain	230.8	144.7	171.1	174.4